Fission Product Yield Calculation by Hauser-Feshbach Statistical Decay and Beta Decay

Shin Okumura[1], *Toshihiko Kawano*[2], *Patrick Jaffke*[2], *Patrick Talou*[2], *Tadashi Yoshida*[1], *Satoshi Chiba*[1]
[1] Laboratory for Advanced Nuclear Energy, Tokyo Institute of Technology, 2-12-1 Ookayama, Meguro-ku, Tokyo 152-8550, Japan
[2] Theoretical Division, Los Alamos National Laboratory, Los Alamos, NM 87545, USA

Abstract

We demonstrate calculations of the prompt neutron emission, the independent and cumulative fission product yield (FPY), decay heat, and delayed neutron yield of ^{235}U(n,f) starting from a set of the primary fission fragment distribution. We employ the recently developed Hauser-Feshbach fragment decay code, HF^{3}D, to calculate the prompt neutron multiplicity and the independent FPY. The β-decay chain of each nuclide in the independent FPY is tracked to obtain the cumulative FPY. The decay heat and delayed neutron yield are calculated by the summation calculation method. Comparisons of the fission and β-decay observables calculated in this work, experimental data, and the evaluated nuclear data libraries provide an important insight for improvements of evaluation of the nuclear data.

1 Introduction

The nuclear fission and decay process of the fission fragment constitute of many different physical phenomena. Due to its complexity, accurate predictions of fission observables by theoretical calculations still remain difficult. At least three processes need to be taken into account for the neutron induced fission of fissile nuclides such as ^{235}U. (1) The formation of compound nucleus, the change of its shape to the saddle-point, and the scission are defined as the process before the scission. (2) After the scission, complementary primary fission fragments are fully accelerated by the Coulomb repulsion and they are highly excited. The fission fragment, which can be characterized by its charge (Z), mass (A), excitation energy (E_x), spin (J), and parity (Π), are then de-excites by emitting the prompt neutrons and photons to reach their ground-state or long-lived isomeric states. (3) The post particle emitted fission fragments, also called fission products (FP), then decay by β-decay leading further delayed neutron and photon emissions.

Due to the very short timescale of the nuclear fission, it makes the direct experimental observation difficult, and very limited experimental information is accessible for (1) to (2). Hence the present evaluation of nuclear data is compiled by combining available experimental data and some phonomenological models, e.g., Los Alamos model (LAM) for prompt fission neutron spectrum [1], Wahl systematics for independent fission product yield (FPY) [2], to supplement scarce experimental data. In addition, such FPY and the other observables are evaluated separately and there are not consistent with each other [3]. There is no certain models and codes that allow us to calculate all of the fission observables simultaneously and consitently from the process (1) through (3). In particular, energy dependence of fission observables has not been well modelled.

In this study, we demonstrate the incident neutron energy dependent calculations of the decay processes of the fission fragment from (2) through (3) starting with the primary fission fragment distribution of ^{235}U(n,f) that characterized by $Y(A, Z, E_{ex}, J, \Pi)$. We discuss the calculated independent and cumulative FPY, decay heats, delayed neutron yields, and their energy dependence compared with the experimental and evaluated nuclear data libraries. We limit our calculation to ^{235}U(n,f) and the incident neutron energy up to 5 MeV, which is the multi-chance fission threshold.

2 Methods

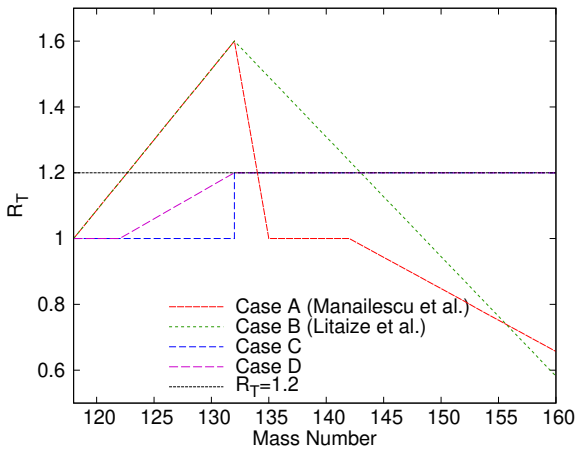

Fig. 1: Variations of the anisothermal parameter R_T as a function of the heavy fragment mass.

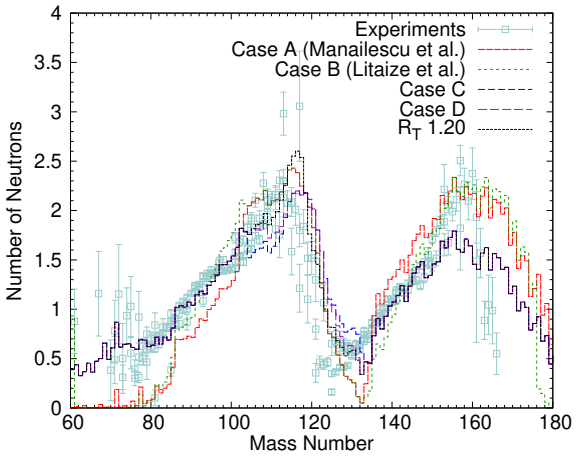

Fig. 2: Comparison of prompt neutron multiplicities of five R_T models.

2.1 Hauser-Feshbach approach

For the de-excitation process of the fission fragments described as (2) in the previous section, a straightforward approach is to apply the Hauser-Feshbach theory to the statistical decay of primary fission fragment pairs. However, the Hauser-Feshbach calculatiion requires many input model parameters. The fission fragment distribtuions are the key ingredients in prompt neutron emission calculations. In order to perform such calculations, one needs to integrate all of the distributions characterizing each of the primary fission fragment. Such integrations have been done by the sampling through Monte Carlo. However, if their distributions have extremely small probability such as FPY, which varies in the order of magnitude typically from 10^{-15} to 10^{-2}, they never samples such cases in a reasonable computation time.

Instead of performing the integration over all probabilities by Monte Carlo sampling, we developed the Hauser-Feshbach Fission Fragment Decay (HF^{3}D) model to calculate various fission observables, i.e., prompt neutron multiplicity ($\overline{\nu}$), independent FPY, and isomeric ratio, simultaneously [4]. The HF^{3}D model performs a numerical integration over the whole ranges of the primary fission fragment yield, their initial excitation energy, spin and parity distributions. In this model, the neutron multiplicities $\overline{\nu}_{l,h}^{(k)}$ are given by integrating the neutron evaporation spectrum $\phi_{l,h}^{(k)}$ from the light or heavy fragment in the center-of-mass system,

$$\overline{\nu}_{l,h}^{(k)} = \int dE_x \sum_{J\Pi} \int d\epsilon \; R(J,\Pi) G(E_x) \phi_{l,h}^{(k)}(J,\Pi,E_x,\epsilon) \; , \tag{1}$$

where $R(J,\Pi)$ is the probability of nucleus having the state of spin J and parity Π, and $G(E_x)$ is the distribution of excitation energy.

2.2 Generation of fission fragment distributions

Scince the general concept of the HF^{3}D model and the generation of the fission fragment distributions have been discussed elsewhere [4], a brief description will be given here. The primary fission fragment yields are generated form the five Gaussians fitted to the experimentally available mass distributions of neutron induced fission of ^{235}U. A charge distribution for each mass is generated by the Z_p model in the Wahl systematics [2]. The total kinetic energy (TKE) as a function of primary fission fragment mass

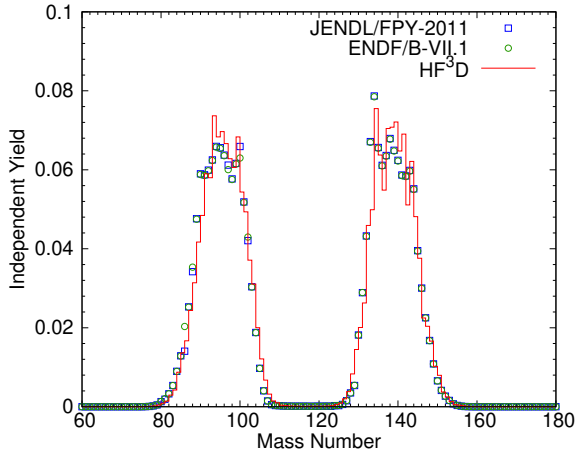

Fig. 3: The mass total of independent FPY of ^{235}U(n$_{th}$,f) calculated by the HF^{3}D model shown with JENDL/FPY-2011 and ENDF/B-VII.1.

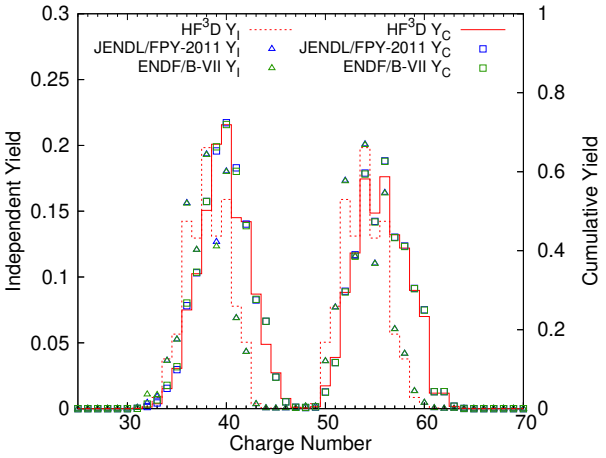

Fig. 4: The charge total of independent(Y_I) and cumulative(Y_C) FPY of ^{235}U(n$_{th}$,f) calculated by the HF^{3}D model with JENDL/FPY-2011 and ENDF/B-VII.1.

is generated based on the fitting an analytical function to the experimental data. The total excitation energy (TXE) can be calculate from TKE by taking into account the energy balance of the reaction. The incident neutron energy dependence of the fission fragment distributions is generated by interpolations of the mass distribution and Wahl's Z_p model.

2.3 Energy sharing between two primary fragments

The evaporating prompt neutrons take away large energy from the primary fission fragments. There is no complete explanations that tells us how the available TXE at a full acceleration is partitioned between two complemental fragments. In the HF^{3}D model, we calculated the energy sharing between the complemental light and heavy fragments by the anisothermal model which is defined by the ratio of effective temperature T_L and T_H of the complemental light and heavy fission fragments expressed as

$$R_T = \frac{T_L}{T_H} = \sqrt{\frac{a_H U_L}{a_L U_H}}, \tag{2}$$

where U is the excitation energy and a is the level density parameter [5]. We took an average value of R_T = 1.2 as previously proposed for ^{235}U(n$_{th}$.f), ^{239}Pu(n$_{th}$.f), and ^{252}Cf(SF) [6, 7].

There exist some different estimates of energy sharing by R_T. Figure 1 shows five cases of different R_T functions. The linear R_T dependence as a function of the heavy fragment mass have been reported for the Spontaneous fission of ^{252}Cf [8] and ^{235}U(n, f) [9] shown as the Case A and B in Figure 1, respectively. Both cases divide minimum excitation energy into the heavy fragment at A_H = 132 because the nuclei with A_H around 132 are almost spherical and the most of deformation energy should be taken by the complementary light fragments. Furthermore, based on the asumption that the symmetrically divided fission fragments should have the same temperatures, we additionally examined two other cases with R_T = 1 around symmetric region. For the case C in Figure 1, R_T = 1 for A_H < 132 and the average R_T for A_H > 132 were used. For the case D, R_T = 1 for A_H < 122, the average R_T for A_H > 132, and linear dependence between A_H = 122 and 132 were used.

2.4 Beta decay

The cumulative FPY can be calculated using the independent FPY by adopting the Bateman equation to each FPs with the decay data library, which contains the radionuclide half-lives and branching ratios.

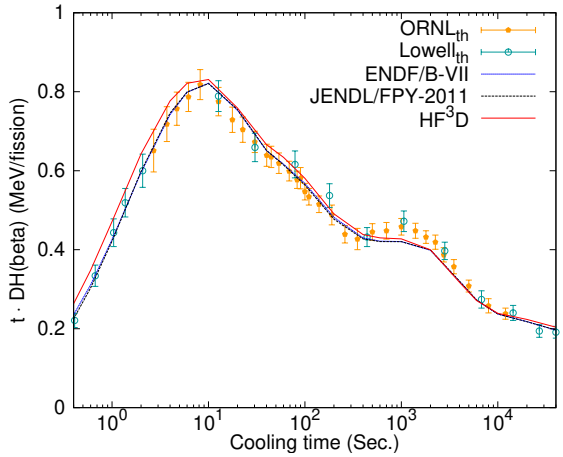

Fig. 5: Decay heat from β emission shown together with experimental data from Lowell and Oak Ridge National Laboratory.

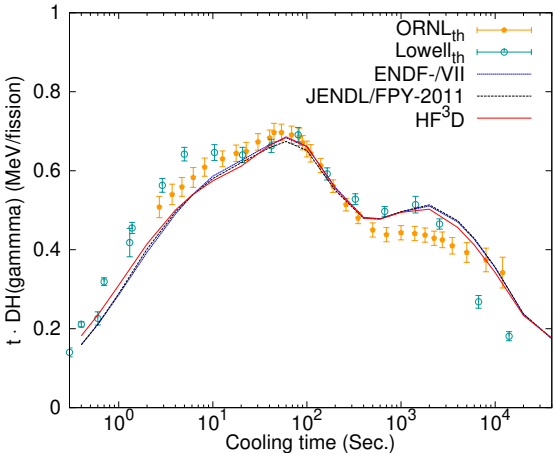

Fig. 6: Decay heat from γ emission shown together with experimental data from Lowell and Oak Ridge National Laboratory.

Suh calculations are performed using a code implemented in HF^{3}D model. The summation calculation predicts aggregate properties of the fission products such as decay heat. The decay heat and the delayed neutron calculations are the sum of the β and γ energies and neutron released from all individual β-decay nuclides [10]. The calculation requires an independent FPY as an input.

3 Results

3.1 Prompt neutron multiplicity

Figure 2 shows the calculated neutron multiplicities ($\overline{\nu}$) of ^{235}U(n$_{\rm th}$,f) as a function of the fission fragment mass for five cases compared with some experimental data [11]. The both of linear R_T functions of [8, 9] show sudden decrease in $\overline{\nu}$ at A_L < 80 and overestimate at A_H > 160. The cases C and D show similar mass dependence of $\overline{\nu}$ compared with the $R_T = 1.2$ case. By comparison with some experimental results [11], the constant $R_T = 1.2$ shows a good agreement with overall mass range. From these results, we concluded that the use of constant R_T for the whole mass range can be quite reasonable for ^{235}U(n$_{\rm th}$,f) case. The average $\overline{\nu}$ for the case R$_{\rm T}$ = 1.2 is 2.38 which is slightly lower than that of the evaluated value 2.41 in ENDF/B-VII.1.

3.2 Independent and cumulative FPY

Figure 3 illustrates the fission product mass dependence of the independent FPY for ^{235}U(n$_{\rm th}$,f). The calculation well reproduce the structures of the independent FPY, seen as peaks (A = 99 and 134) and dips (A = 98 and 136). These fine structures can be seen in both ENDF/B-VII and JENDL/FPY-2011 libraries. The peaks at A = 99 and 134 are due to the high production ratio of ^{99}Zr and ^{134}Te, respectively, and the isobar productions in the same mass. The calculated independent FPY reproduces not only the case with higher production yield region but also very low yield regions down to 10^{-15}.

The cumulative FPY was obtained by performing the β-decay calculation using the calculated independent FPY. Since the β decay and the following delayed neutron emission hardly affect the mass yield, the masses of FP are mostly governed by the independent FPY. We thus compare the charge distribution of FPY before and after β decay. As shown in Figure 4, the charge distribution of the independent FPY has quite clear even-odd effect and the mass distribution of the cumulative FPY shows the clear shift towards the heavy charge. A relatively large discrepancy appears at Z = 41 (Nb). This is mainly due to a treatment of long-lived FP in the decay chain. In our β-decay calculations, we treat

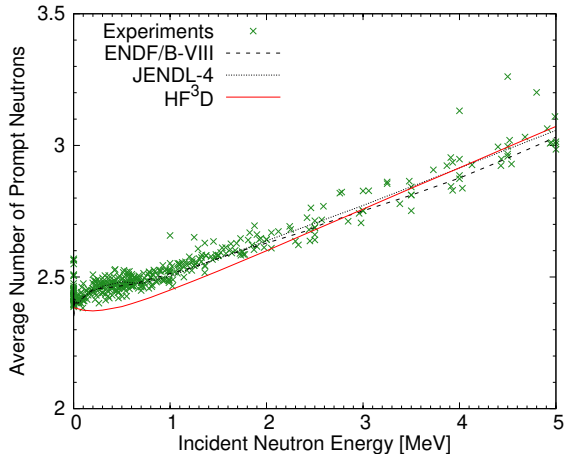

Fig. 7: Energy dependence of calculated prompt neutron multiplicity.

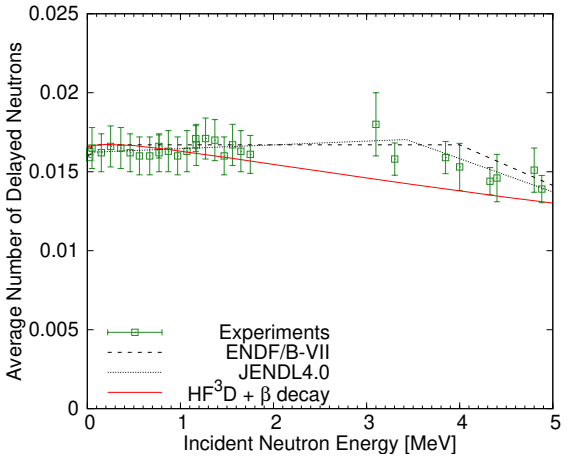

Fig. 8: Energy dependence of calculated delayed neutron yield.

the fission products with half-lives longer than 1,000 years as stable nuclides. JENDL/FPY-2011 and ENDF/B-VII treat ^{93}Zr ($T_{1/2}$ = 1.61 $\times$ 10^6 years) which is the β-decay precursor of ^{93}Nb. However, the overall appearance of the calculated cumulative FPY shows a good agreement with ENDF/B-VII and JENDL/FPY-2011 libraries.

3.3 Summation calculation

The β- and γ-energy components in the decay heat were obtained separately. Figure 5 shows the decay heat multiplied by the cooling time from the fission burst as a function of t. The calculated decay heat from the β emission agrees with the experimental data from Lowell and Oak Ridge National Laboratory [12,13]. The major differences occurred in the decay heat from the γ emissions below 10 second after the fission burst. By comparing with the cases using independent FPY of JENDL/FPY-2011 and ENDF/B-VII, ^{97g}Y is highlighted to the cause of the overestimating. In this study, any of adjustments were introduced at each calculation steps. For the better evaluation of FPY, more detailed investigation on the starting distribution and introducing some adjustments would be required.

3.4 Energy dependence of prompt and delayed neutron emissions

The number of emitted neutrons obviously play a main role for governing the fission product yields in both prompt and delayed emissions. Figure 7 shows the incident neutron energy dependence of the prompt neutron multiplicity calculated with the HF^{3}D model compared with the experimental data. Below 1 MeV, our results show an opposite tendency to experimental and evaluated data, however, the differences are still quite small. On the contrary, the number of the experimental data of the delayed neutron emission yields (ν_d) are less sufficient in particular between 1.5 and 5 MeV. Figure 8 shows the incident neutron energy dependence of ν_d compare with JENDL-4.0 and ENDF/B-VII. The HF^{3}D model calculations are approximately follow the experimental data below 5 MeV. In both evaluated libraries, ν_d slightly increase up to around 4 MeV and sharply decrease above 4 MeV. This sharp decrease is attributed to the effect of the multi-chance fission.

4 Conclusion

The independent FPY of ^{235}U(n,f) is calculated with the HF^{3}D model by applying the Hauser-Feshbach theory to the fission fragment decay. The cumulative FPY, the decay heat and delayed neutron are also calculated by the β decay calculation and the summation calculation using the calculated independent

FPY as an input. We demonstrated the calculations of the fission observables such as independent and cumulative FPY, $\overline{\nu}$, and ν_d simultaniously and consistently starting from one fission fragment distribution. These fission observables were reproduced reasonably well comparing with experimental data and evaluated nuclear data libraries.

We extended our calculation up to 5 MeV where the multi chance fission takes place. The incident energy dependence of $\overline{\nu}$ and ν_d was compared with experimental data and evaluated nuclear data libraries. Although there are some discrepancies between the calculated and experimental results, the overall predictions are quite successful. This method should be a quite powerful tool for evaluating fission observables in the future.

5 Acknowledgeents

This work was partially supported by the grant 'Development of prompt-neutron measurement in fission by surrogate reaction method and evaluation of neutron- energy spectra,' entrusted to JAEA by Ministry of Education, Culture, Sports, Science and Technology. This work was partly carried out under the auspices of the National Nuclear Security Administration of the U.S. Department of Energy at Los Alamos National Laboratory under Contract No. DE-AC52-06NA25396.

References

[1] David G. Madland and J. Rayford Nix. New calculation of prompt fission neutron spectra and average prompt neutron multiplicities. *Nuclear Science and Engineering*, 81(2):213–271, 1982.

[2] A. C. Wahl. Systematics of fission-product yields. Technical Report LA-13928, Los Alamos National Laboratory, 2002.

[3] Patrick Jaffke. Identifying inconsistencies in fission product yield evaluations with prompt neutron emission. *Nuclear Science and Engineering*, 190(3):258–270, 2018.

[4] S. Okumura, T. Kawano, P. Jaffke, P. Talou, and S. Chiba. ^{235}U(n, f) independent fission product yield and isomeric ratio calculated with the statistical Hauser-Feshbach theory. *Journal of Nuclear Science and Technology*, 0(0):1–15, 2018.

[5] T. Ohsawa, T. Horiguchi, and H. Hayashi. Multimodal analysis of prompt neutron spectra for ^{237}Np(n,f). *Nuclear Physics A*, 653(1):17 – 26, 1999.

[6] P. Talou, T. Kawano, and L. Bonneau. Prompt fission neutrons as probes to nuclear configurations at scission. *AIP Conference Proceedings*, 1005(1):198–201, 2008.

[7] P. Talou. Advanced modeling of prompt fission neutrons. *AIP Conference Proceedings*, 1175(1):261–268, 2009.

[8] O. Litaize and O. Serot. Investigation of phenomenological models for the monte carlo simulation of the prompt fission neutron and γ emission. *Phys. Rev. C*, 82:054616, Nov 2010.

[9] C. Manailescu, A. Tudora, F.-J. Hambsch, C. Morariu, and S. Oberstedt. Possible reference method of total excitation energy partition between complementary fission fragments. *Nuclear Physics A*, 867(1):12 – 40, 2011.

[10] K. Oyamatsu, H. Takeuchi, M. Sagisaka, and J. Katakura. New method for calculating aggregate fission product decay heat with full use of macroscopic-measurement data. *Journal of Nuclear Science and Technology*, 38(7):477–487, 2001.

[11] K. Nishio, Y. Nakagome, H. Yamamoto, and I. Kimura. Multiplicity and energy of neutrons from 235U(nth,f) fission fragments. *Nuclear Physics A*, 632(4):540 – 558, 1998.

[12] J.K. Dickens, T.A. Love, J.W. McConnell, and R.W. Peelle. Fission-product energy release for times following thermal-neutron fission of ^{235}U between 2 and 14000 s. *Nuclear Science and Engineering*, 74(2):106–129, 1980.

[13] S. Li. Beta decay heat following ^{235}U, ^{238}U and ^{239}Pu neutron fission. *Ph.D. thesis*, 1997.